

Camera for recording light backscattered from textured photovoltaic samples

Antonio Parretta

ENEA Centro Ricerche Portici, Località Granatello, I-80055 Portici (Na), Italy

E-mail: parretta@portici.enea.it

Received 6 November 2002, accepted for publication 5 June 2003

Published 22 August 2003

Online at stacks.iop.org/JOptA/5/S284

Abstract

A camera for recording the intensity of light backscattered from textured photovoltaic (PV) samples is described. It was realized by modifying a professional folding camera, for use on an optical bench. The collimated light from a laser source crosses the camera and impinges on the test sample. The light backscattered by the sample exposes a punched photographic plate placed on the front side of the camera. With a proper choice of laser light intensity and wavelength, the optical diffusing effects produced by surface morphology or by subsurface features of the sample can be recorded in this way. The analysis of light diffusing characteristics of textured PV samples, mainly based on crystalline silicon material, can be directed towards improving their light collection capabilities. The camera can be assembled in such a way as to record the light diffusion images produced in reflection by both small and large samples, or those produced in transmission from textured semitransparent materials.

Keywords: Light scattering, recording, textured silicon, photovoltaic devices

1. Introduction

Semiconductor surface texturing is a common practice in the fabrication process of photovoltaic (PV) devices, in the view of improving their light collection capabilities [1–4]. The effect produced by texture is to scatter the incident light into the bulk semiconductor, allowing longer light paths therein and, consequently, higher chances for absorption, particularly for longer wavelengths. Also, the reflectance at the surface is greatly reduced by surface texture due to the multiple reflections allowed to the incoming beam and the consequent increase of absorption probability. The efforts to improve light collection capabilities of PV devices, by adopting the most efficient texturing designs, have greatly increased in the modern silicon cell technology, as the actual tendency is to reduce cell thickness down to a few tens of microns.

Light scattering into the semiconductor has, as a counterpart, the light backscattering from the sample towards the source hemisphere of part of incident light. The analysis of this backscattered light has not been extensively investigated until now [5]. It could bring new information about the light collection process and new ideas about technological solutions for improving it, as backscattered light can be viewed as a sort

of ‘image’ of light diffused into the semiconductor, deformed by the particular structure of the surface texture. Recent studies performed at ENEA on textured silicon samples [6–9], indeed, have demonstrated a correlation between aspect ratio of the backdiffused light, which quantitatively describes the extension of light diffusion, and light collection (absorption) efficiency. It appeared evident from the published data that the shape of diffused light, weighted with its intensity, is correlated with the amount of light collected by the sample.

Techniques for analysing the light scattered by a surface, generally applied to the determination of roughness parameters, are well established [10]. These techniques use photodetectors for measuring total or angle-resolved scattered radiation. If the knowledge of polarization of the scattered radiation is not required, simple and fast methods can be set up for detecting the spatial distribution of the scattered radiation intensity. Several methods have also been developed by ENEA for visually inspecting, measuring and recording the backscattered light [6–9].

In this paper, we present a simple optical apparatus making use of a professional folding camera for recording the angular distribution of scattered light [11, 12]. The apparatus also comprises a laser source and optical components

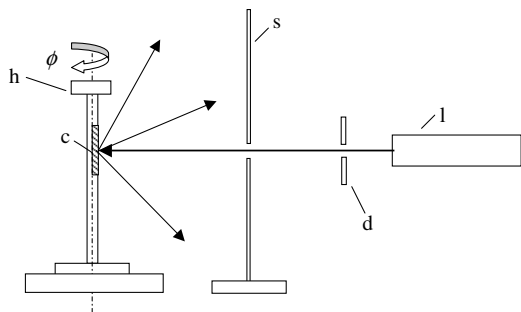


Figure 1. Experimental set-up, comprising a pierced planar screen, for visualizing the light backscattered by a sample.

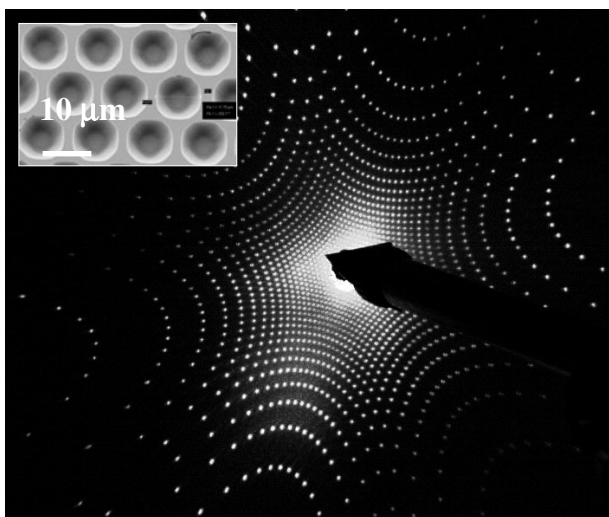


Figure 2. Photograph of the light pattern (LBI) produced at $\lambda = 543 \text{ nm}$ by a silicon sample textured by hemispherical wells in a honeycomb structure (see the box).

for spatially and temporally controlling the incident light. The photographic plate inside the camera faces the scattering surface and collects part of the total scattered light. Several features of the camera allow us to change the angle of incidence of light on the sample and angular extent of backscattered light recording. The developed film becomes a useful and practical support for saving the optical information. The optical scanning of the film and the image elaboration at the computer can be finally used to get quantitative information about the scattered light intensity distribution.

The use of the camera for recording light forward diffused by semitransparent textured samples is also presented and discussed.

2. Light scattering from textured PV samples

Depending on the structure of surface texture, the light backscattered from a textured sample gives rise to different types of light pattern, or scattering images, hereinafter called LBIs (light backscattering images) for short. The visualization of LBIs by any of the methods described below generally precedes the process of recording by the camera. The visualization step is necessary to have a quick estimate of the light intensity angular distribution and then to choose the most appropriate configuration for the camera: sample–film

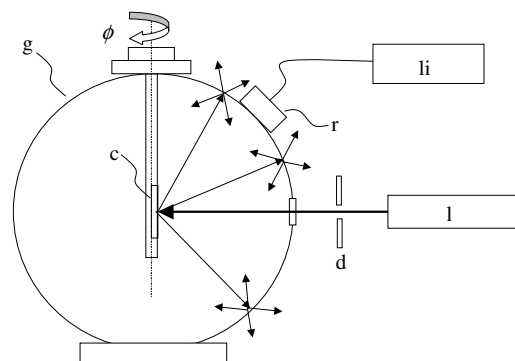


Figure 3. VISAGE scatterometer (visualizing scattering globe) made of a sandblasted plastic, semitransparent globe, used for both visualizing and measuring the scattered light intensity distribution. For only measuring purposes, it is not necessary to sandblast the globe.

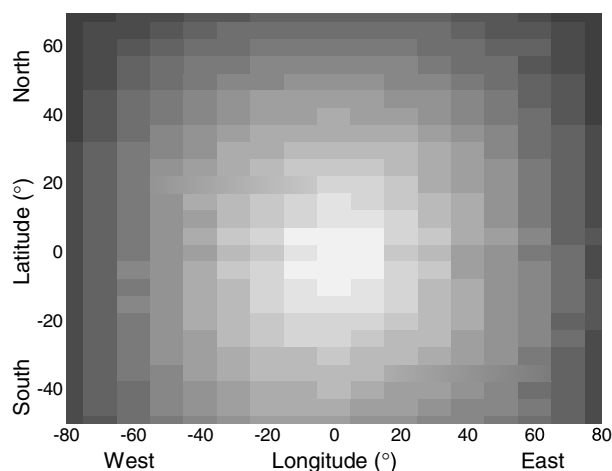


Figure 4. LBI of a porous silicon sample, measured at $\lambda = 633 \text{ nm}$ by moving a silicon photodetector along the longitude and latitude lines drawn on the globe of the VISAGE scatterometer (see figure 3).

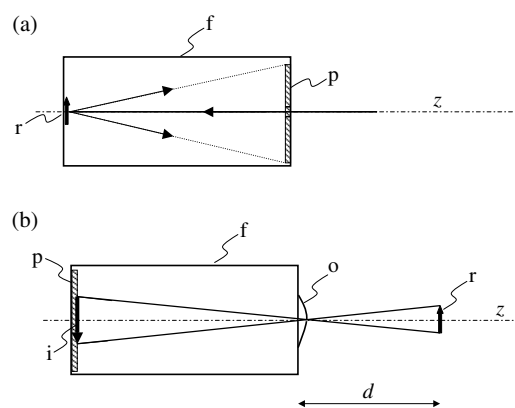


Figure 5. Operating principle of the CARDIFF (backscattering) camera with planar plate (a). It is compared with the operating principle of the normal (refraction) camera (b).

distance, angle of incidence of the light beam on the sample, parallelism between sample and film etc. To visualize the LBI in a quick and simple way, we used white and pierced screens, of plane or cylindrical geometry, placed between the laser source and the sample, in order to have the scattering

figure reproduced on them. Figure 1 shows the experimental set-up consisting of a laser source (l), a diaphragm (d), a pierced planar screen (s) and a sample holder (h) for holding and rotating the sample (c) around the vertical axis. Figure 2 shows the LBI produced with the set-up of figure 1, at $\lambda = 543$ nm, by a silicon sample textured by hemispherical wells distributed on a honeycomb array [3]. An LBI with clearly distinct maxima of intensity is obtained, as the sample is textured by a regular spatial distribution of wells on the surface, and the light intensity distribution follows the laws of diffraction. As an alternative, plastic globes with the sample placed at the centre can be used (see figure 3). In this case the globe (g) is transparent to laser light and the internal wall can be sandblasted in order to allow the scattering, and then the visualization, of the light backscattered by the sample (c) [8, 9]. The use of a photodetector (r) moved over the globe surface also allows us to have a rough estimate of backscattered light intensity distribution, and then to use the apparatus as a scatterometer. Randomly textured samples produce a backscattered light which is angularly dispersed in a continuous way in the front hemisphere. This can be seen in figure 4, where the LBI of a stain-etched porous silicon sample [8, 9], obtained by moving a silicon photodetector along the longitude and latitude lines drawn on the globe of the VISAGE scatterometer, is shown. The backscattered light intensity, in this case, follows the laws of Lambert for the emission of light from ideal diffusers [13].

3. The 'CARDIFF' apparatus

3.1. Introduction

The operating principle of the apparatus for recording backscattered light, or simply the backscattering camera, hereinafter called 'CARDIFF' (camera for recording diffused and diffracted light images), is schematically shown in figure 5(a) and is compared with the normal 'refraction' camera of figure 5(b) [11, 12]. In figure 5(b), the object (r) is external to the camera (f) and, through the objective (o), produces an image (i) on the backside of (f) where the photographic plate (p) is placed. The distance d between object and objective is related to the focal length of the objective. In figure 5(a), in contrast, the object is placed on the backside of the camera (f) and the backscattering image (LBI) is reproduced on the photographic plate at the front side of (f). In figure 5(a) the LBI can be recorded at any distance from (r) as no focal distance is present. Whereas the object (r) is reproduced inverted on the image (i) in the refraction camera, in the scattering camera it is the Fourier transform of the surface structure that is reproduced on the LBI.

The films used for exposure to backscattered light are to be chosen depending on the laser light wavelength and on the intensity of light diffused by the sample on the film. Films of the 'orthochromatic' type are used for wavelengths in the 400–580 nm range (blue–green–yellow), whereas films of the 'panchromatic' type are to be used for wavelengths $\lambda > 580$ nm (red).

3.2. Light backscattering from small samples

The simplified schematic view of the 'CARDIFF' apparatus, to be used for recording light reflected from small samples, is

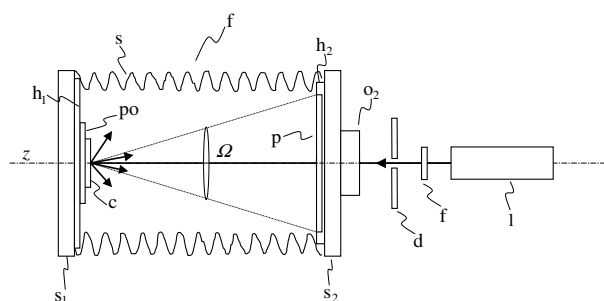


Figure 6. Schematic view of the CARDIFF apparatus configured for light backscattering recording on small samples.

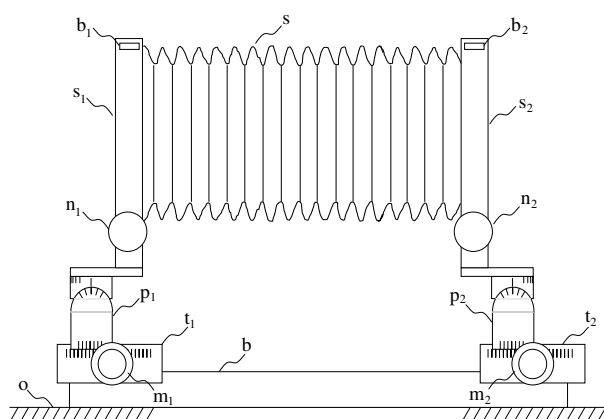


Figure 7. Schematic lateral view of the CARDIFF camera.

Components: (o) optical bench; (b) track; (t_1) and (t_2) slides; (m_1) and (m_2) locking knobs; (p_1) and (p_2) goniometers; (n_1) and (n_2) knobs for vertical translation; (s_1) and (s_2) walls; (b_1) and (b_2) spirit levels; (s) bellows.

shown in figure 6 [11, 12]. The apparatus is mounted on a rail and fixed on an optical bench. The source of light is a laser with wavelength λ . The light intensity at input of the camera is regulated by the neutral filter (f) and the light beam is spatially selected by the diaphragm (d). By operating on the shutter (o_2), the exposure time t_0 can be preset. The light pulse crosses the punched plate (p), mounted on the chassis (h_2), fixed on the wall (s_2), and the camera (f), striking the surface of sample (c), placed on the sample holder (po), mounted on the chassis (h_1), fixed on the wall (s_1). The backscattered radiation intercepted within the collecting solid angle Ω reaches the photographic plate (p). Light outside Ω is absorbed by the bellows and does not interfere with light recording. The solid angle Ω can be varied by translating the walls (s_1) and (s_2) along the optical axis z . The maximum value for Ω is dictated by the bellows (s), when they are totally compressed. High values of Ω , however, are undesirable as they imply too low glancing angles on points of the film far from the optical axis, with consequent high light reflection and low exposure (see appendix). Problems related to contrast uniformity can be reduced by adopting a different geometry for the camera, as will be discussed in section 3.5.

A schematic lateral view of the camera alone is shown in figure 7. The camera was realized by suitably modifying a professional folding camera for an optical bench. The camera is fixed on two slides, (t_1) and (t_2), which can translate over the track (b), fixed on the optical bench (o). By moving the slides the distance between sample (c) and plate (p) can be

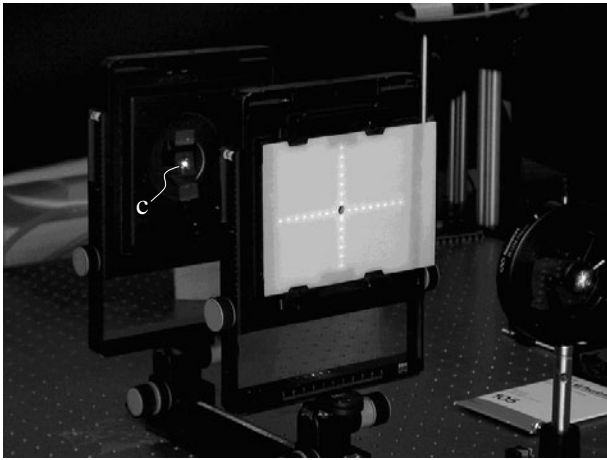


Figure 8. The camera is shown open in the dark during the alignment procedure. The LBI produced on the frosted glass screen by a PERL cell is visible. (c) is the illuminated sample.

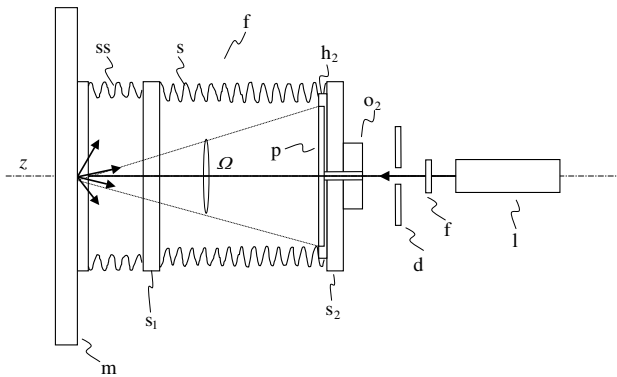


Figure 9. Schematic view of the CARDIFF apparatus configured for light backscattering recording on large samples.

varied. Each slide is provided with a rack where the supports (p_1) and (p_2) can be finely moved and locked by knobs (m_1) and (m_2). Other knobs can be used for the fine translation of the walls (s_1) and (s_2) horizontally and vertically along the two axes orthogonal to the optical axis z . The wall (s_2) is made of an extractable part, a chassis (h_2) that holds the pierced plate (p) on the internal side and the shutter (o_2) on the external side. Extracting a ‘volet’ from the chassis (h_2), the plate (p) is exposed to the light inside the camera and the hole (~ 10 mm diameter) on the plate is cleared for the passage of the laser beam and the plate (p) is exposed to the light inside the camera. The mechanical shutter (o_2) allows us to set the exposure time t_0 , typically from 1/500 to 1 s. Besides the translation movements, the two walls, (s_1) and (s_2), can be rotated around a vertical and a horizontal axis to adjust the parallelism between walls (s_1) and (s_2) and their orthogonal orientation with respect to the optical axis z .

For recording the LBI of small samples, first of all, the laser (l) is aligned with respect to the optical axis z (see figure 6). The two walls (s_1) and (s_2) are then aligned by acting on the knobs shown in figure 7. A more precise alignment of the walls can be made by centring the LBI on a frosted glass screen, pierced at the centre and fixed on the wall (s_2) in place of the photographic plate (see figure 8). After the alignment procedure, the camera is closed by the bellows (s)

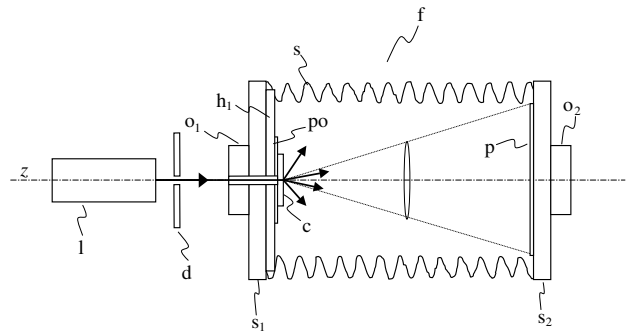


Figure 10. Schematic view of the CARDIFF apparatus configured for light forward scattering recording on small samples.

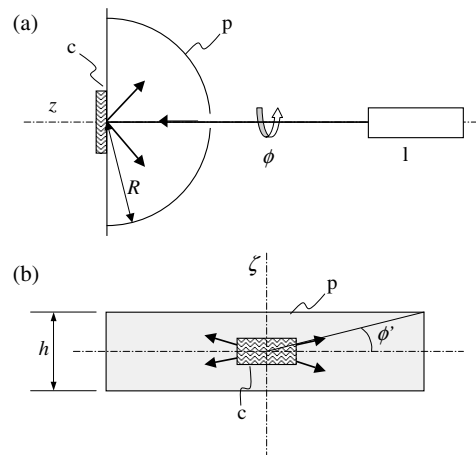


Figure 11. Simplified schematic drawing of the CARDIFF apparatus with cylindrical geometry. (a) Top view; (b) backside view.

and the recording procedure can start. The chassis (h_2) is charged with a pierced film and mounted on wall (s_2), and the ‘volet’ is open. After the exposure, the ‘volet’ is closed and the extractable chassis (h_2) is removed from (s_2).

3.3. Light backscattering from large samples

By minor modifications of the backside, the CARDIFF camera can be adapted for recording light backscattered from large samples, such as single solar cells of large dimension (typically 10–12 cm) or even solar cells mounted on PV modules. Figure 9 shows the schematic view of the modified camera. The chassis (h_1) is removed and supplementary bellows (ss) are inserted on the wall (s_1), connecting in such a way the camera, fixed on the optical bench, to the sample (m). Large samples like PV modules are mounted on a separate translation stage which is put beside the optical bench. The camera is then translated along the rail in such a way as to reach the module (m) by means of the bellows (ss). The procedure for recording light remains the same as that described in the previous section.

3.4. Light scattering through small semitransparent samples

By reversing the source position and by adding a new shutter on the backside, the CARDIFF camera can be adapted to operate to record the forward scattered light from small semitransparent samples, like textured TCO (transparent

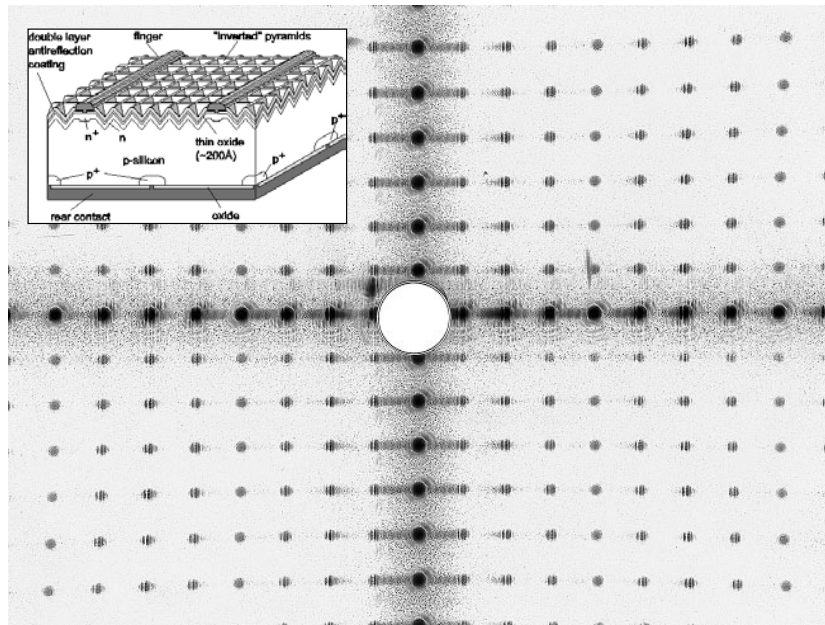


Figure 12. LBI of a single-Si sample textured with a square array of inverted pyramids (sample no 4 in table 1).

conducting oxide) coatings deposited on glass. These samples are frequently used as window materials on the front side of PV cells made from not-crystalline silicon semiconductors (a-Si, CIS etc), and are intentionally textured to forward scatter light within the semiconductor and then to increase light absorption efficiency [14]. In order to investigate the efficiency of TCO texturization with respect to the forward diffusion of incident light, the use of the CARDIFF camera in transmission turns out to be very appropriate. Figure 10 shows a schematic view of the camera modified for recording the scattered light in transmission. The laser source (l), filter (f) and diaphragm (d) are mounted on the backside of the camera. A new shutter (o_1) is mounted on the wall (s_1). The chassis (h_1) is modified in order to have the sample holder (po) pierced to allow the passage of the laser beam. The light diffused by the sample (c) is collected by the film within the solid angle Ω , as for the case of backscattering recording.

3.5. CARDIFF camera with non-planar geometry

The problems related to spatial non-uniformity of the contrast on the film can be reduced by adopting a geometry for the camera different from the planar one, for example by using a cylindrically shaped collecting film, as adopted in the photographic powder techniques of x-ray crystallography. The cylindrical configuration has the advantage of being easily realized as it requires simply to bend the film on a suitable support. Figures 11(a), (b) show the schematic views of the cylindrical camera in which the film is bent to cover a semicircumference. In this case the distance from sample (c) to film (p), R , is constant for a horizontal collecting plane, orthogonal to the axis ζ of the cylinder (azimuth $\phi = 0$). This allows us to have a constant and normal incidence of light on the film surface for all the points intercepted on the film by that plane. Moreover, the film is able to collect light reflected at angle α between -90° and 90° . If the film tape width h is not too large, this condition can be assumed valid for most of the

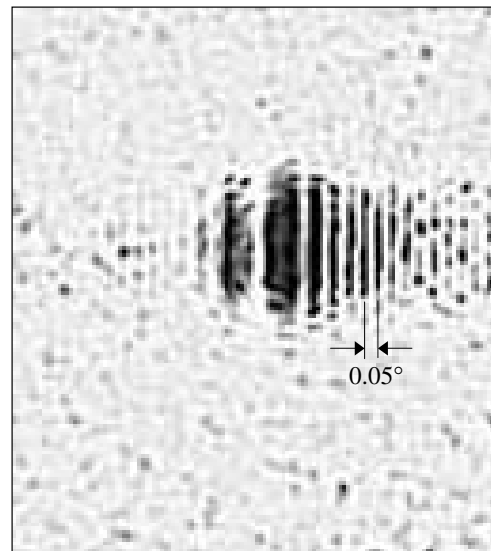


Figure 13. Detail of the LBI of the sample of figure 12.

diffused rays from the sample. If the horizontal plane is rotated around the optical axis z of angle ϕ (see figure 11(b)), we have that, for $\phi < \phi' = \tan^{-1}(h/2R)$, diffused light is collected from $\alpha = -90^\circ$ to $+90^\circ$. For $\phi > \phi'$, the maximum angle α for collection of diffused light will decrease to the value $\alpha = \tan^{-1}(h/2R)$ in correspondence to the azimuth angle $\phi = 90^\circ$.

4. Characterization of textured samples

The apparatus 'CARDIFF' was extensively used to characterize different types of PV sample. Here we will report the results of light scattering recording in reflection mode from both small and large samples. A He-Ne laser, unpolarized, with $\lambda = 632.8$ nm and $P = 25$ mW, was used. The

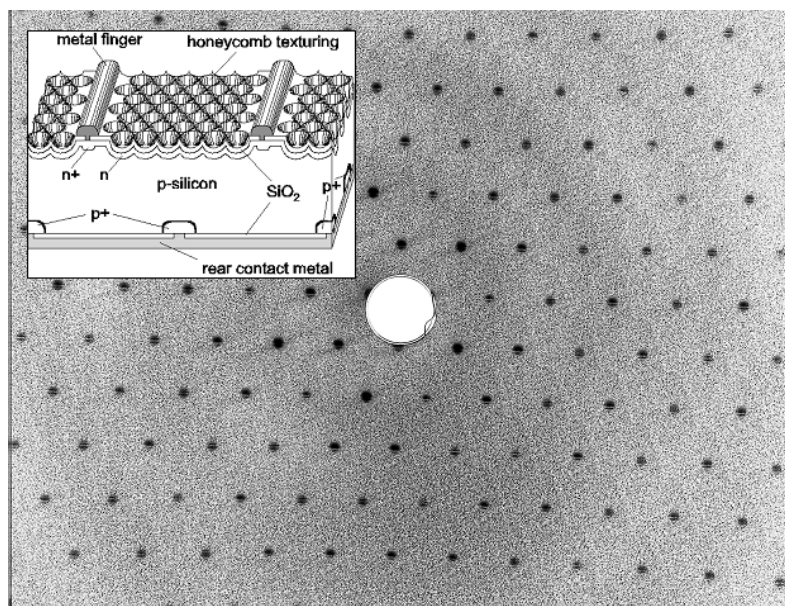


Figure 14. LBI obtained with a multi-Si sample textured with a hexagonal array of hemispherical wells (sample no 5 in table 1).

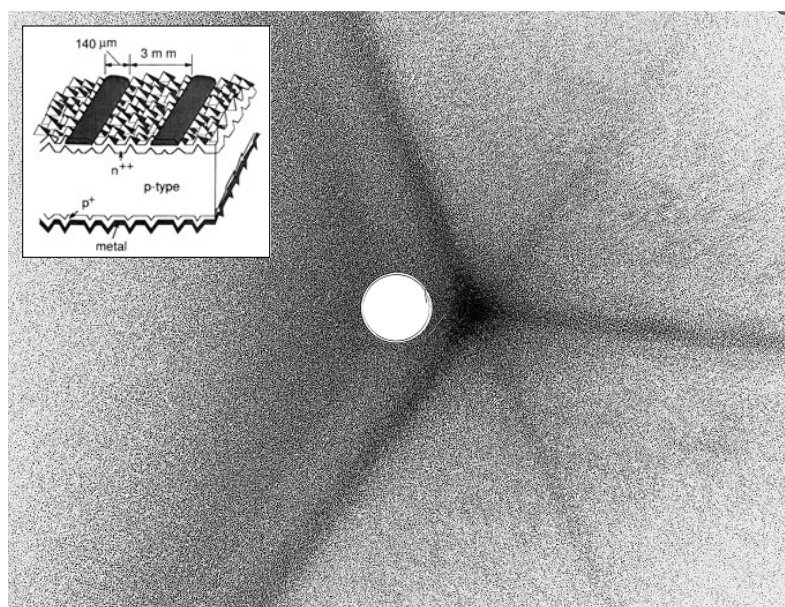


Figure 15. LBI of a multi-Si sample textured with upright pyramids randomly distributed on the surface (sample no 8 in table 1).

small samples were 1–2 cm in size. Large samples were ~ 1 square foot crystalline silicon modules from the University of New South Wales [15]. Photographic plates with dimension $12.5 \text{ cm} \times 10 \text{ cm}$ ($12 \text{ cm} \times 9.5 \text{ cm}$ exposed area) were used. The photographic images were obtained exposing Kodak T max 100 and Kodak Technical pan films. The relatively short wavelength, with low penetration depth in silicon, and the high thickness of samples ($100 \mu\text{m}$), allowed only the near surface backscattering to be recorded. The backscattering information, therefore, mainly refers to the surface texture of samples. The distance, d , between sample (c) and film (p) was fixed at 17 cm, and then $\Omega \sim 0.4 \text{ sr}$. Silicon samples with different surface textures were characterized (see table 1). They were realized by either texturing silicon wafers or realizing a

complete textured PV device. The samples can be roughly divided into three classes. The first class comprises samples textured with a regular array of texture features [2, 3]. The regular array is obtained by using photolithographic processes. They produce LBIs that are the result of diffraction phenomena, and appear with clearly distinct, intense light spots toward precise directions in space, as previously illustrated in figure 2. The second class comprises samples textured with randomly distributed features, like square upright pyramids [16]. They produce no diffraction patterns due to the absence of a regular structure, but only the effects of multiple reflections on the four faces of the small pyramids can be observed. The third class comprises the samples that have a random surface texture, such as the porous silicon samples. They produce scattering

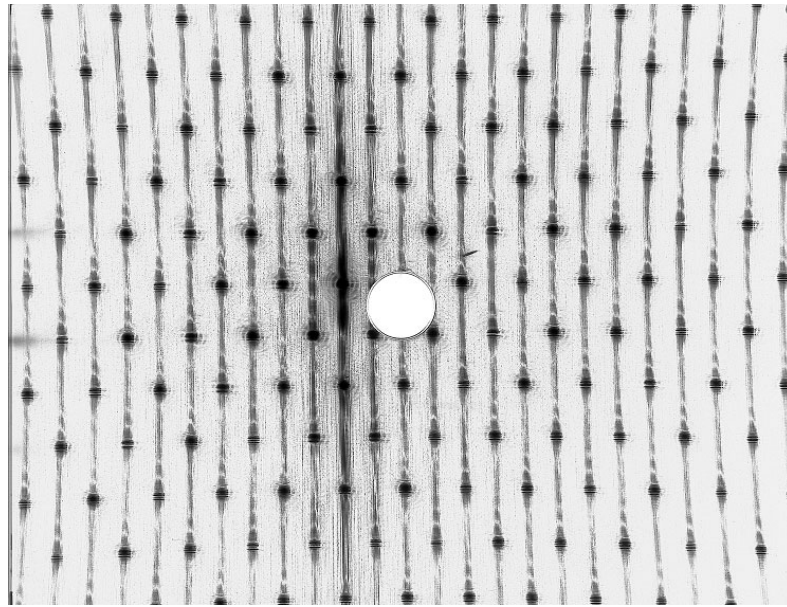


Figure 16. LBI of a multi-Si sample textured by hemispherical wells. The laser beam impinges on the metal grid.

Table 1. List of the characterized samples, with the type of surface texture indicated. An indication of where the laser beam is impinging is also given.

No	Sample	Texture	Notes
1	PERL	Inverted pyramids	Beam on grid
2	PERL	Inverted pyramids	Beam on Si
3	PERL	Inverted pyramids	Beam on grid
4	PYR	Inverted pyramids	Beam on Si
5	HC	Hemispherical wells	Beam on Si
6	HC	Hemispherical wells	Beam on grid
7	HC	Hemispherical wells	Beam on grid
8	m-Si	Upright pyramids	Beam on grid
9	p-Si	Nanoporosity	Beam on Si
10	PERL module	Inverted pyramids	Beam on grid
11	PERL module	Inverted pyramids	Beam on grid

figures with a quite regular intensity distribution in space, due to the excellent diffusion properties of this material and to the small size of surface porosities with respect to λ (see figure 4). Table 1 reports the sample characteristics and the modality of light recording. In particular, it is indicated where the light beam is impinging: whether only on the semiconductor surface or also on the contact metal grid.

In the following we will present and discuss only the most interesting and representative scattering figures obtained from the samples of table 1. Figure 12 shows the negative of the best LBI obtained with samples textured by inverted pyramids at normal incidence of the laser beam (sample no 4 in table 1). The inverted pyramids are obtained by anisotropic etching of (100) oriented silicon wafers [2]. The regular square array of the texture (see the box in figure 12) is reproduced on the LBI. The main spots in the cross can be analysed to precisely calculate the base size of the pyramids, Δs , by applying the Bragg equation: $\Delta s \sin \theta = k\lambda$, with k integer. Figure 13 shows a detail of the LBI, with the internal structure of a light spot evidenced. The interference fringes are appreciable down to $\sim 0.05^\circ$, corresponding to a distance of $\sim 150 \mu\text{m}$ on the

film. A better resolution is prevented by the coarse grain of the developed film. Figure 14 shows the negative of the LBI obtained with samples textured by hemispherical wells, always at normal incidence (sample no 5). The wells are obtained by isotropic etching of multi-crystalline silicon substrates [3]. The regular hexagonal (honeycomb) array of the texture (see the box in figure 14) is reproduced on the LBI. Figure 15 shows the negative of the LBI obtained with samples textured by upright pyramids (sample no 8) [16]. This texture is obtained by anisotropic etching of the (100) Si surface, and produces pyramids randomly distributed on the surface (see the box), with dispersed dimension, but all equally oriented in space. The LBI then shows the effect of light multiple reflections from the four faces of the pyramids. The disturbing effect produced by the light scattering from the metal grid can be appreciated by looking at the LBI of figure 16. It was obtained by analysing sample no 6.

5. Conclusions

A camera for recording, on a photographic support, the LBI of diffused or diffracted light by textured PV samples has been presented. The camera, called CARDIFF, can operate in reflection with both small and large samples, and in transmission with small semitransparent samples. For all these cases the different configurations taken by the camera have been illustrated. The CARDIFF apparatus is realized by using a laser and a professional folding camera for operation on an optical bench, modified as described in the text. Planar or cylindrical geometries can be used. In reflection mode, the laser beam crosses the camera, impinges on the opaque textured sample and is backdiffused, and a portion of it illuminates the film for a prefixed exposure time. In transmission mode, the laser beam impinges on the semitransparent textured sample, is forward diffused and a portion of it illuminates the film for a prefixed exposure time. The camera with planar geometry is widely discussed in

this work. By means of this, different LBIs from both small and large textured PV samples have been recorded by using a laser with $\lambda = 633$ nm wavelength. The quality of the records and the resolution reached turned out to be excellent. The use of a scanner operating on the 'negative' film, or on the 'positive' film reproduction, allows us to quantitatively analyse the images and to extract important information on the geometry of the diffusing textured surfaces. Measurement of the reflectance properties of the photographic paper is in progress, as it would improve the precision of the above quantitative analysis.

Appendix. Analysis of backscattered light records (planar geometry)

A quantitative analysis of backscattered light can be performed only if a correct choice of exposure conditions, that is intensity of incident radiation and exposure time, is made. These conditions are to be optimized by making preliminary calibration measurements in order to operate, as closely as possible, in the linear range of the curve density of developed image versus exposure.

In the following, we present a theoretical approach for the correction of density as a consequence of the different angles of incidence of light on the different points of the photographic plate. Figure A.1 shows the schematic optical path of light diffused by the sample (c) at angle α and impinging at the same angle α on the film (p) at distance r . As the flux of light diffused at angle α within a unitary solid angle is constant, the irradiance measured at normal incidence along the direction of vector \vec{r} , $G(r)$, is given by

$$G(r) = G(r_0) \cdot (r_0/r)^2 \quad (1)$$

where r_0 is a reference distance on the vector \vec{r} . The irradiance of light absorbed by the film (p) at point P can be expressed, therefore, as

$$G_{abs}(r, \lambda) = \text{constant} (1/r^2) \cos^3 \alpha [1 - R(\alpha, \lambda)] \quad (2)$$

where $R(\alpha, \lambda)$ is the reflectance of the film at angle of incidence α and wavelength λ . Introducing the distance d between sample and film along the optical axis, we obtain

$$G_{abs}(d, \alpha, \lambda) = \text{constant} (1/d^2) \cos^3 \alpha [1 - R(\alpha, \lambda)]. \quad (2')$$

As we can see from equation (2'), the density of radiant energy absorbed at a particular point of the film strongly changes at changing angle α , as it depends on the inverse of the cube of $\cos \alpha$. The consequence of this result is that points on the film far from the optical axis are less exposed to light. This fact can give problems when a quantitative analysis of the film contrast is performed. Equations (2) and (2') give simplified expressions for the absorbed irradiance. We should take into account, in fact, that the film is changing during exposure, and then the reflectance factor depends on time t ($0 \leq t \leq t_0$):

$$G_{abs}(d, \alpha, \lambda, t) = \text{constant} (1/d^2) \cos^3 \alpha [1 - R(\alpha, \lambda, t)]. \quad (3)$$

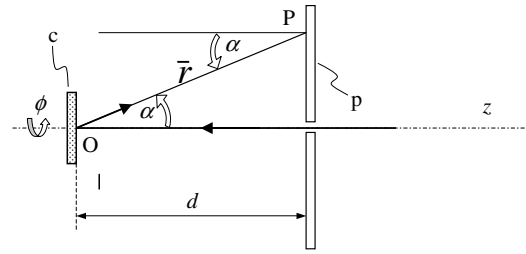


Figure A.1. Schematic optical path of a light ray diffused by a sample (c) at angle α , impinging at angle α on the film (p).

By considering the average reflectance of the film during exposure time t_0 , the average irradiance can be given by

$$\bar{G}_{abs}(d, \alpha, \lambda, t_0) = \text{constant} (1/d^2) \cos^3 \alpha [1 - \bar{R}(\alpha, \lambda, t_0)]. \quad (4)$$

At a first approximation, the film reflectivity can be assumed constant with respect to angle α , and then the final expression for the absorbed irradiance could be

$$\bar{G}_{abs}(d, \alpha, \lambda, t_0) = \text{constant} (1/d^2) \cos^3 \alpha [1 - \bar{R}(\lambda, t_0)]. \quad (5)$$

The irradiance of equation (5) is directly related to the degree of exposure of the film, and then to the measured density, as long as the film exposure conditions are such that no saturation effects are present. A quantitative analysis of the contrast on the film, measured by a scanning process and a subsequent elaboration at the computer, has therefore to take into account equation (5) for the light absorbed by the unitary surface. To complete this analysis, a confirmation of the assumption made about the constancy of film reflectance with angle should be made. The direct measurement of reflectance of the film at different wavelengths and angles is, therefore, an important subject for a future work.

References

- [1] Green M A 1995 *Silicon Solar Cells, Advanced Principles and Practice* (Sydney: Centre for Photovoltaic Devices and Systems, UNSW) pp 92–116
- [2] Zhao J, Wang A, Altermatt P and Green M A 1995 Twenty-four percent efficient silicon solar cells with double layer antireflection coatings and reduced resistance loss *Appl. Phys. Lett.* **66** 3636–8
- [3] Zhao J, Wang A, Green M A and Ferrazza F 1998 19.8% efficient 'honeycomb' textured multicrystalline and 24.4% monocrystalline silicon solar cells *Appl. Phys. Lett.* **73** 1991–3
- [4] Green M A and Wenham S R 1995 Silicon cells: single junction, one sun, terrestrial, and single and multiple crystalline *Solar Cells and Their Applications* ed L D Partain (New York: Wiley) pp 55–78
- [5] Bawolek E J, Mohr J B, Hirleman E D and Majumdar A 1993 Light scatter from polysilicon and aluminium surfaces and comparison with surface-roughness statistics by atomic force microscopy *Appl. Opt.* **32** 3377–400
- [6] Bobeico E, Varsano F, Roca F and Parretta A 2001 Characterization of textured silicon surfaces by light backscattering measurements *Proc. Int. Conf. on Materials Science and Condensed Matter Physics (Chisinau, Moldova, July 2001)* p 212
- [7] Parretta A, Bobeico E, Nasti I and Varsano F 2002 Lightbackscattering analysis of textured silicon samples *1st aSi-Net Workshop–8th Euroregional Workshop on Thin Silicon Devices (Salerno, Italy, March 2002)*

-
- [8] Parretta A, Bobeico E, Lancellotti L, Morvillo P, Wang A and Zhao J 2002 Analysis of light backscattering from textured silicon surfaces *PV in Europe, from PV Technology to Energy Solutions* (Rome, Oct. 2002)
- [9] Parretta A, Bobeico E, Lancellotti L, Morvillo P, Wang A and Zhao J 2003 A new approach to the analysis of light collected by textured silicon surfaces *3rd World Conf. on Photovoltaic Energy Conversion* (Osaka, May 2003)
- [10] Bennet J M and Mattsson L 1999 *Introduction to Surface Roughness and Scattering* (Washington, DC: Optical Society of America)
- [11] Parretta A and Granata S 2001 Apparecchio per la riproduzione della figura di diffusione della luce da campioni fotovoltaici *Patent It Application N. RM 2001 A 000576 24*
- [12] Parretta A 2002 Camera for recording light backscattered from textured photovoltaic samples *19th Congr. Int. Commission for Optics ICO XIX Optics for the Quality of Life* (Firenze, Aug. 2002) vol 4829 ed A Consortini and G C Righini (Firenze: SPIE) pp 831–2
- [13] Kortum G 1969 *Reflectance Spectroscopy, Principles, Methods, Applications* (Berlin: Springer)
- [14] Anna Selvan M J A 1999 ZnO for thin film solar cells *Thesis* Université de Neuchâtel, Neuchâtel
- [15] Zhao J, Wang A, Campbell P and Green M A 1999 22.7% efficient silicon photovoltaic modules with textured front surface *IEEE Trans. Electron Devices* **46** 1495
- [16] Green M A 1995 *Silicon Solar Cells Advanced Principles and Practice* (Sydney: Centre for Photovoltaic Devices and Systems, UNSW) pp 201–33